Chair of Spacecraft Systems
TUM School of Engineering and Design
Technical University of Munich

Designing a Future Space-based Communication Infrastructure

From Demand Forecasting for Space Communication Networks to Assessing Architectures through Tradespace Exploration

Jonas Heiderer
TUM School of Engineering and Design, Technical University of Munich
jonas.heiderer@tum.de

December 1, 2024

Abstract — The rapid expansion of digital technologies and the Internet of Things has lead to exponential growth in global data traffic, exposing the limitations of terrestrial communication networks by addressing growing demands for high-speed, low-latency connectivity, especially in remote areas. Low Earth orbit satellite constellations have emerged as a promising solution, offering reduced latency and global coverage compared to traditional geostationary systems. This paper addresses key questions related to the design and implementation of a scalable space-based communication infrastructure. A predictive demand model is developed to evaluate future requirements for global coverage and connectivity. Based on these requirements, an architecture model simulates a tradespace of potential configurations, which are analyzed to maximize coverage while minimizing costs, considering technical and launch constraints. Results indicate that an X-band constellation at 600 km orbital altitude and 90° inclination offers the best coverage-to-cost ratio. However, the high number of satellites required necessitates increased launch capacities to fully meet future demand. Additionally, combining various orbital configurations and employing advanced data handling techniques could enhance data rates per satellite and reduce technical challenges.

1 Introduction

In the current Information Age, characterized by the rapid growth of digital technologies and global connectivity, the demand for high-speed, reliable internet access has become a fundamental aspect of modern society. As digitization permeates nearly every facet of daily life, the need for a robust communication infrastructure capable of supporting these demands is increasingly critical. The rise of the Internet of Things (IoT), with its potentially billions of connected devices, has further intensified this need, leading to an exponential increase in data traffic [1] and placing immense pressure on existing terrestrial communication networks. This paper investigates the demand for future global connectivity and analyzes architectural choices for space-based communication infrastructures using a tradespace analysis.

1.1 Motivation

Traditional internet infrastructure, primarily reliant on fiber-optic cables and ground-based wireless networks, has been remarkably effective in connecting much of the global population. However, this infrastructure faces significant limitations, particularly in remote and underserved regions where laying fiber-optic cables is economically unfeasible. Furthermore, as data rates continue to increase, driven by applications such as streaming services, cloud computing, and real-time interactive technologies, the capacity of terrestrial networks is being pushed to its limits. These challenges are compounded by the growing demand for low-latency communication, which is crucial for emerging technologies like autonomous vehicles and real-time data processing in IoT applications. In this context, the development of space-based communication infrastructure, particularly in Low Earth orbit (LEO), offers a compelling alternative to conventional internet systems. LEO satellite constellations, such as those being deployed by SpaceX's Starlink [2] and OneWeb [3], have the potential to provide global, high-speed internet coverage, bypassing the geographical and infrastructural constraints of ground-based networks. These systems can offer significantly lower latency compared to traditional geostationary satellites, making them well-suited for latency-sensitive applications. Additionally, the flexibility and scalability of LEO constellations allow them to adapt to the growing demand for bandwidth (BW) and connectivity, ensuring that even the most remote areas can be connected to the digital world. The motivation for

establishing a space-based communication infrastructure is driven not only by the need to expand global internet access but also by the growing reliance on digital technologies in everyday life. As the world becomes increasingly interconnected, the ability to provide reliable, high-speed internet to all corners of the globe will be essential in supporting economic growth, bridging the digital divide, and fostering innovation in both developed and developing regions. Moreover, the ongoing digital transformation, accelerated by the proliferation of IoT devices and the increasing integration of artificial intelligence into various sectors, necessitates a communication infrastructure that can handle vast amounts of data efficiently and securely [4], [5]. With the rapid advancements in satellite technology, including the miniaturization of satellites, improvements in launch capabilities, and the development of inter-satellite links (ISL), space-based systems are becoming more cost-effective and capable of meeting the demands of the digital age. As such, the deployment of a space communication infrastructure is poised to play a pivotal role in the future of global connectivity, ensuring that the benefits of the digital revolution are accessible to all.

1.2 Background

The development of communication infrastructure has evolved significantly since the inception of modern networking technologies. Starting with the introduction of the Advanced Research Projects Agency Network (ARPANET) in the late 1960s, which pioneered packet-switching technology, communication systems have continuously advanced to meet increasing global demands [6]. This laid the groundwork for the World Wide Web in the 1990s, revolutionizing connectivity and enabling the widespread adoption of the internet. As internet access became commercially available, global connectivity surged, with the number of internet users exceeding 5 billion in 2023 [7]. Concurrently, the demand for bandwidth has grown exponentially, driven by the proliferation of data-intensive applications. Terrestrial networks, primarily based on fiber-optic cables and wireless systems, have since been the cornerstone of global connectivity. Despite significant advancements in terrestrial communication infrastructure, including the deployment of 5G networks promising ultra-low latency and higher data rates, challenges such as geographical limitations and the high cost of infrastructure expansion remain. To overcome these constraints, space communication infrastructure has played an increasingly vital role.

A space critical infrastructure comprises the physical asset, the satellite and the orbit, in which the asset operates [8]. Communication satellites have been in service since the 1960s, providing niche services, for example acting as relays for long distance broadcasts and providing positioning and synchronization services for mobile terrestrial communication systems. Commonly, these large satellites have been placed in geosynchronous orbits at approximately 36000km above the earth's surface with near zero inclinations, allowing earth-based antennas to remain permanently pointed at the satellite due to its apparent almost stationary position in the sky [8]. In recent years, there has been a renewed focus and an ever-increasing interest in small low earth orbit (LEO) satellites due to the growing demands for high data rate applications, massive connectivity and universal internet access [9]. Development cost, launch cost and propagation delays of small LEO satellites are significantly lower than of the traditionally heavyweight and large MEO and GEO satellites. However, capabilities and resources of a single small satellite are limited, which is why a network of small satellite is required to fulfill the task [9]. The initial set-up cost of such dense small satellite networks will be huge, and low-earth orbits will not only impact the expected lifetime of satellites due to atmospheric drag. Collision avoidance would require careful orbital planning, and de-orbiting of non-functional satellites can also become a challenge with growing satellite populations [9]. Nonetheless, these networks will put huge amounts of communication resources in space that could benefit various terrestrial communication systems. Advantages are its wide area coverage and reducing latency by lowering round-trip times due to its lower orbital altitudes. The sheer number of satellites also leads to a lower user per satellite ratio, being able to handle an order of magnitude more devices. Additionally, offloading data from terrestrial networks could be enabled and overloading avoided, increasing the resilience of the overall communication network [9].

The main functions of a space communication system are in general receiving and transmitting data from and to earth, as well as receiving and transmitting data from and to other satellites. The two types of communication that are typically used are radio frequency (RF) and free space optical (FSO), also referred to as laser communication [10]. RF communications for spacecraft are conducted between 30 MHz and 60 GHz, divided up into frequency bands of certain BW. The lower frequencies are typically more mature for

small satellites, however extensive use of these bands has led to crowding and challenges for acquiring licensing. Higher frequency bands are more susceptible to atmospheric attenuation and lead to a higher free space loss, but offer a better ratio of gain-to-aperture-size [10]. While BW is the limiting factor for any satellite constellation, atmospheric attenuation is the main external factor affecting the link performance. Since high-speed optical links used between satellites are not used for ground-links because of frequent cloud interference [11], RF links are the norm. In order to maximize the spectral efficiency under current weather conditions, adaptive modulation and coding schemes are commonly used [12]. Due to the higher frequencies used in FSO, the amount of BW available for communicating is much larger compared to RF which enables much higher data rates [10]. In addition, optical space data links are faster than terrestrial links because there is no time delay in free space like there is in fibers [10]. Laser communication between satellites can cross thousands of kilometers in a straight line compared to the often circuitous routes of terrestrial fiber paths [10], which is why FSO is an interesting concept for ISL.

1.3 Paper Research Questions and Objectives

This paper is trying to answer the following research questions:

- How can a predictive demand model be used to design a scalable, space-based communication infrastructure that meets the future requirements of global coverage and connectivity?
- Which space-based architecture maximizes coverage while minimizing costs?
- How can such an infrastructure be implemented, considering technical and launch constraints required to ensure its feasibility?

In order to be able to answer these research questions, the paper's objectives and goals are as follows: Firstly, to create a predictive model to forecast and simulate the demand for future space communication and understand potential challenges and opportunities. Secondly, to utilize the developed model to analyze the future demand deeply and propose multiple scalable space communication infrastructure based on distinctive figures of merit. Thirdly, to analyze and find the most efficient architecture constellation in terms of coverage and related costs, and lastly, to analyze the technical feasibility and realizability to understand the challenges of implementation.

1.4 Paper Structure

After giving an introduction in the first section of this paper, describing the motivation and providing background information to the topic, section 2 shortly discusses the methodology that has been used for this problem and the primary and main assumptions are listed. Section 3 explains the workflow of the model that has been developed. Section 4 summarizes the link budgets, section 5 discusses the results and validates the model. Finally, after a short outlook on next steps and further studies to be conducted is given, section 7 concludes the paper summarizing the most important results and answering the research questions.

2 General Methodology

This section presents the integrated approach that has been used to characterize the tradespace of a space-based communication infrastructure. An overview of the methodology is shown in the functional flow block diagram illustrated in Fig. 1. The approach is structured in five steps, namely Preparation, Enumeration, Simulation, Evaluation, and Selection. These steps are further decomposed in sub-steps, to better understand and follow the structure of this work.

2.1 Preparation

After establishing a general foundation and defining the scope of this work, it was considered which steps need to be followed in order to propose a design for a space infrastructure. Firstly, an infrastructure must meet the demand of its main purpose, in this case the communication infrastructure must be able to cover the demand of global BW. Now the discussion arises to what extent this demand must be met, which ideally should be 100% in order to make full use of the advantages compared to ground-based infrastructures. After identifying and collecting relevant statistical data of the past decades, a forecast model was established. The future growth was estimated using existing methods, such as curve fitting and making use of the sigmoid function. The best fitted curve that was also in accordance with other forecasts and could be validated by result comparison was chosen for the further process. In order to be able to perform a tradespace

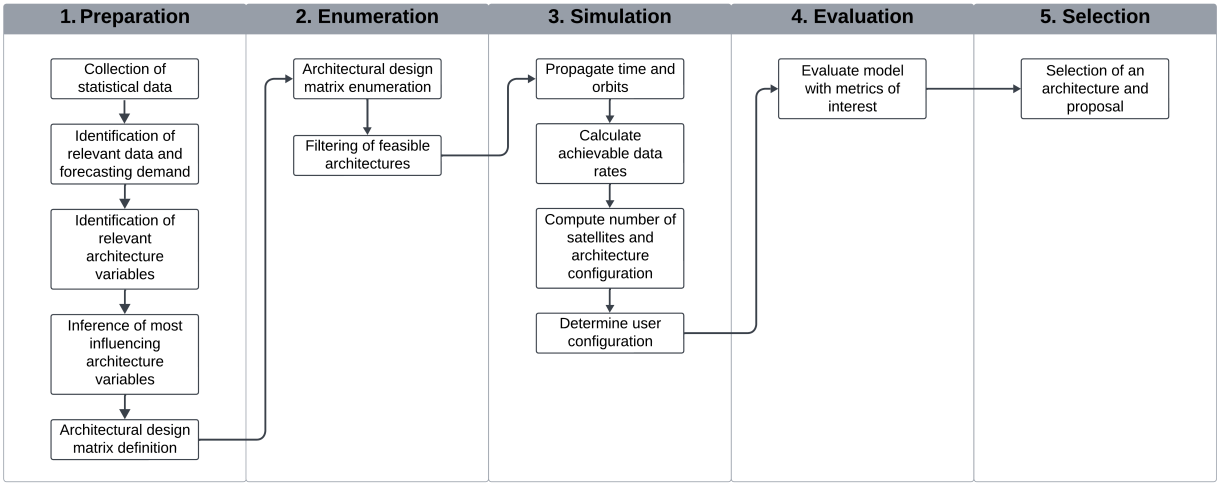

Figure 1 Flow chart describing the general methodology.

exploration on a future space communication infrastructure a set of interconnected decision variables is defined. To clearly establish the orbital configuration of such a space infrastructure, the average altitude and the inclination will be considered. Furthermore, different frequency bands have been considered for communication. The decision variables can be found in the morphological matrix Table 1.

As one of the objectives of this thesis is to provide a low-latency global infrastructure for communication, different LEO orbits are considered, namely 300, 600, 900 and 1200 km. In addition, the objective of providing high coverage supports the choice to include the orbital inclination in the design process. According to [13] more than 50% of the population is located between 30° north and south, with 45° inclination more than 75% of the population can be served, with 60° more than 95% and with 90° full coverage is achieved. Assuming circular orbits simplifies the model by standardizing orbital distance, although in reality, minor eccentricity variations could influence coverage intervals. Lastly, the most common frequency bands for satellite communication have been considered. Due to the fact that downlink is the bottleneck of a space-based infrastructure, only the frequencies feasible for downlink were considered, namely S, X, Ku, and Ka. V-band was included in the link budget for completeness, even though it does not represent a feasible solution. The choice of the bands comes with a set of parameters typical in respective space applications. For simplicity, further assumptions are made. Assuming unlimited satellite capacity and optical ISLs enhances flexibility in data relay and minimizes latency, although practical constraints could necessitate additional relay satellites or ground stations for higher inclinations. In addition, optical ISLs are still conceptual and additional communication terminals in all directions would be required, drastically increasing system complexity. Because of that, the chosen type of communication as well as the orbital altitude decide on the amount of satellites required to satisfy a given demand. Depending on this number, the RAAN (Right Ascension of Ascending Node) is chosen in a way that enables equal distribution in orbit and equal distances between satellites, both adjacent within an orbit and adjacent in orbital planes.

2.2 Enumeration

The scope of step 2 is to define all the feasible architectures that are contained within the architectural design matrix. Each combination of the decision variables represents a unique system architecture in the tradespace. For a fixed demand a total of 64 configurations are theoretically possible, which are listed in Table 2. Following enumeration, constraints are imposed to rule out infeasible combinations, and eventually obtain a set of possible architectures which are successively analyzed later on.

2.3 Simulation

The next step comprises the simulation of every defined architecture. This is done by providing the decision variables as input to the created model, which runs the simulation to first compute achievable data rates,

Table 1 Architectural Design Matrix

Architectural decisions		**Decision alternatives**			
Option ID		1	2	3	4
Orbital configuration	Altitude [km]	300	600	900	1200
	Inclination [°]	30	45	60	90
Communication	Frequency band	S	X	Ku	Ka

Table 2 Architectural Configurations

Option ID	**Altitude [km]**	**Inclincation [°]**	**Frequency**
1	300	30	S
2	300	30	X
3	300	30	Ku
4	300	30	Ka
5	300	45	S
...	...	...	...
64	1200	90	Ka

then determine a possible satellite configuration, and finally a user configuration.

2.4 Evaluation

The architecture configurations will be evaluated according to multiple primary metrics. Firstly, the number of satellites plays an important role. Not only is it a limiting factor of feasibility due to launch capacities and constraints, but increasing numbers also have a negative effect on safety, reliability, sustainability and affordability [14]. Furthermore, operational costs, impacted by satellite count and frequency band selection, can significantly influence the feasibility of configurations. Higher frequencies like Ka-band enable higher data rates but often require more complex and costly ground infrastructure [15]. Secondly, the population coverage provided by the constellation is used to determine the utility of the configuration, keeping in mind that one of the objectives is to provide a high coverage communication infrastructure. Thirdly, latency reduction is integral to user experience, particularly in low-altitude orbits. Configurations with lower altitudes reduce signal travel time, thereby optimizing latency and meeting the goal of a low-latency infrastructure. Lastly, as the demand for data rate per user increases, scalability considerations become critical. Higher data rates require significantly more satellites, particularly at high inclinations, impacting both the operational cost and technical complexity of the constellation. Combined, these metrics make up an evaluation of efficiency and effectiveness of the constellation, helping to choose the appropriate technology and hardware for the further design process.

2.5 Selection

As a final step an exclusion process is used to identify the architectures with the most efficient trade-offs across the metrics of interest. Resulting from this, architectures of interest are identified for a more detailed design study. The approach presented here identifies architectures for serving a set of predefined customers and covering a predefined demand. In order to validate the model and to gain insights on the architectural problem, already existing communication infrastructures such as SpaceX's satellite constellation Starlink were used.

3 Assumptions

Assumptions were made to simplify the tradespace exploration, focusing on the feasibility and effectiveness of different orbital and communication configurations. They are collected in Table 3.

4 Modeling

The overall model compromises several smaller models, that have been eventually put together and work as one. They are interdependent to some extent and their way of operation will be explained in this chapter.

Table 3 Made assumptions with their description.

Assumption	Description
Circular Orbit	Orbits are assumed to be circular, minimizing variability in distance from Earth's surface.
Similar Orbits	No combinations of diverse types of orbits are assumed.
Unlimited Capacity	Satellites are assumed to simultaneously handle all incoming and outgoing communication.
Optical ISLs	Satellites are assumed to connect freely, reducing latency and relay limitations.
Global Demand	The entire global demand is assumed to be handled by the satellite constellation.
No Progress	It is assumed that mankind's technological capabilities do not advance.

4.1 Demand Model

To begin with the demand model, Fig. 2 depicts the workflow logic on which the system was built. As a first step historical data on different categories has been collected, which could be used to develop a forecast and predict future values. To give an example of the first row, the category *global internet users* was considered. Data sets were collected on *internet users* as well as *population* before computing the *penetration depth*. This resulted in a forecast for *global internet users*, which could be further specified to *peak global users*. In a similar manner the other two categories were handled. The forecast of *devices per capita* multiplied with the *global internet users* suggests how many total devices will be connected. Another forecast estimates how many of the *connected devices* are part of the IoT, and how many are high data rate devices such as mobile phones. The final category *data rates* compares the forecast of *global BW* with the computed value. This value is obtained by forecasting *data rate per phone* and multiplying this value with the previous value for *connected devices*. It also includes different use cases to give an idea what activities leads to which amount of BW.

4.2 Architecture Model

The workflow of the architecture model is depicted in Fig. 3. As a first step, with the input *orbital altitude*, a *link budget* can be computed for RF and FSO communication. This provides us with the *achievable downlink data rates per satellite*. Furthermore, with said input and the assumption of a circular polar orbit the *latency* for a roundtrip to the ground and back, as well as for an ISL can be computed. For the next step, two different approaches were chosen: For the second approach, the minimum number of satellites required to achieve total global coverage is computed. This was done according to the equations presented in [11]. Continuing from this point, the global network capacity can be computed, as well as the BW per user and the downlink data rates to ground stations or directly to the end user. Nevertheless, since the focus of this paper is on satisfying the estimated demand, this approach is neither further discussed, nor displayed in the workflow. In the first approach, the *total number of satellites* can be computed by dividing the *network capacity* by the *achievable data rates per satellite*. The global BW, in other words the *network capacity*, is obtained from the demand model Fig. 2. In the final category *users*, a value for the *inclination* is given as input which determines the *total users per satellite*. With the *network capacity* given, the *BW per user* can be calculated, resulting in a *user configuration*.

4.3 Overall Model

Finally, the workflow of the overall model is described in Fig. 4. After defining the architectural variables for a satellite constellation, a communication model (link budget) and a demand model were created independently. Next these single models were integrated in the final model and represent inputs to the architectural model. Each block was validated independently, and if the output is not desirable or not plausible, the input can be refined and adapted. Once validated, the complexity of the overall model was increased, and a similar validation process was applied. The final output represents a proposal to a space-based communication infrastructure.

5 Communication

In this section the results of the conducted link budgets in RF and FSO communication are presented and discussed. For the sake of comparison of every type of communication, it was chosen to first list the results at the same altitude. While downlink budgets were computed at 600 km altitude, the slant range in between adjacent satellites at this orbital height is approximately 2720 km for the ISLs. It is important to mention that the slant range will decrease with increas-

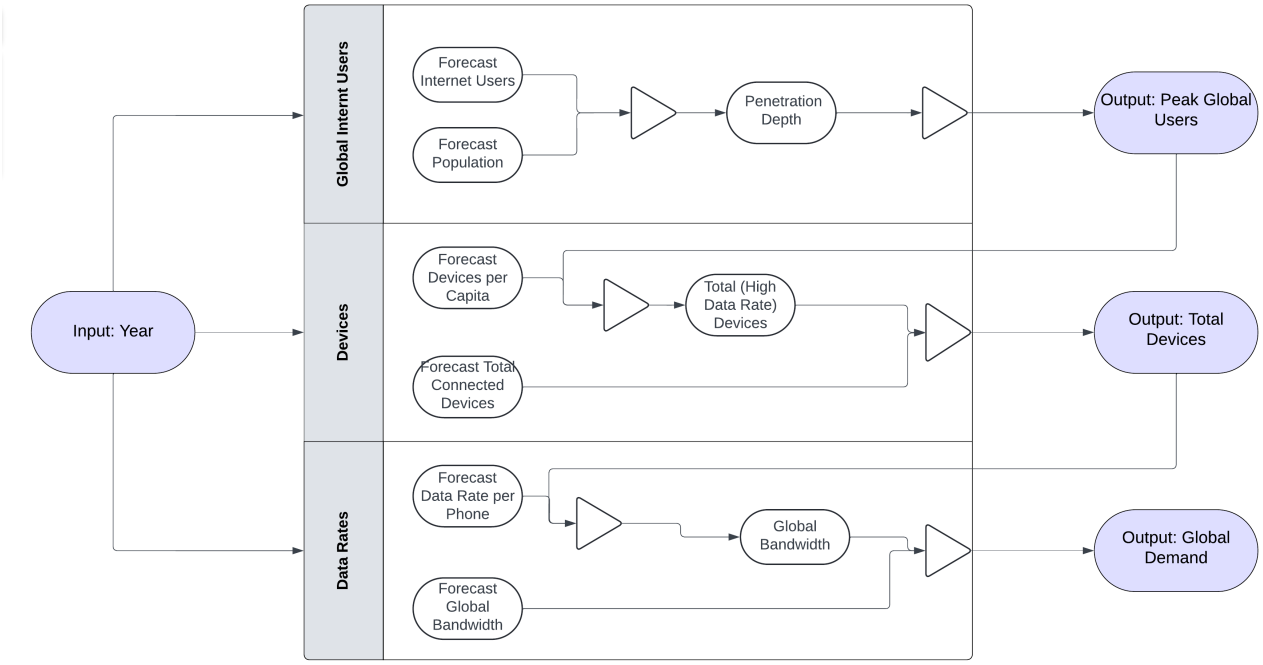

Figure 2 Flow chart describing the workflow of the demand model.

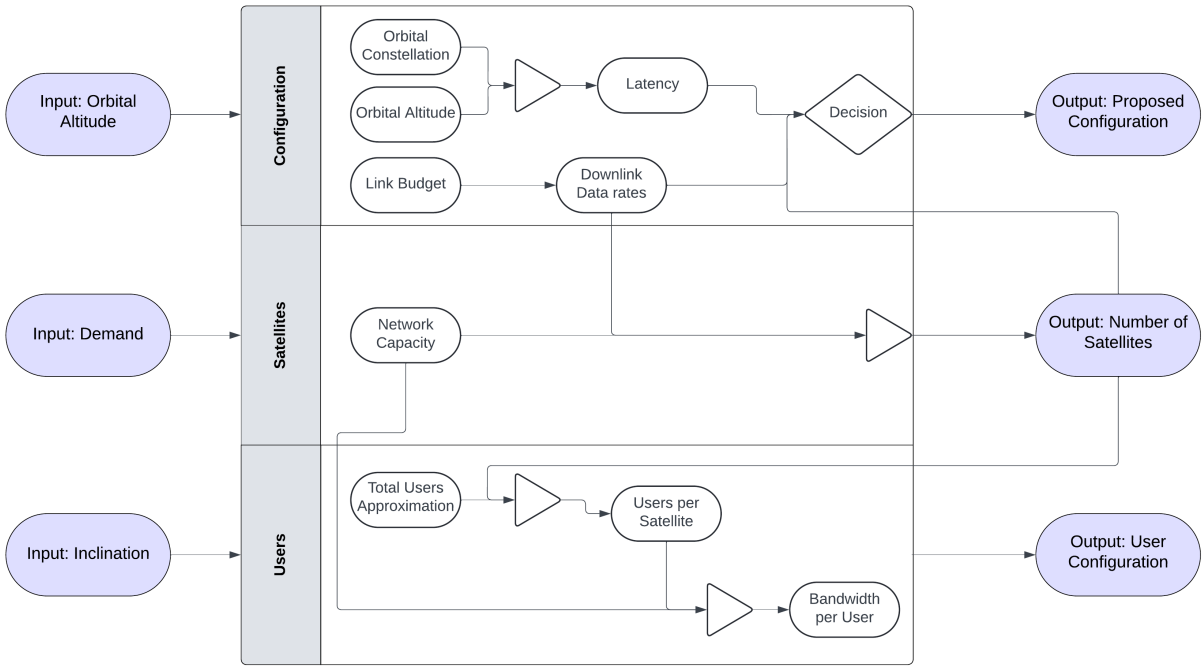

Figure 3 Flow chart describing the workflow of the architecture model.

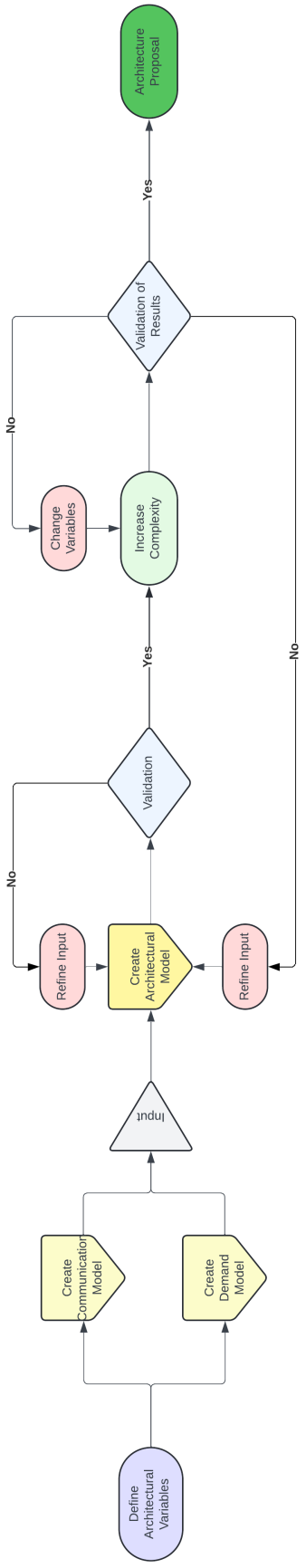

Figure 4 Flow chart describing the workflow of the overall model.

Band	Frequency
VHF	30 to 300 MHz
UHF	300 to 1000 MHz
L	1 to 2 GHz
S	2 to 4 GHz
C	4 to 8 GHz
X	8 to 12 GHz
Ku	12 to 18 GHz
K	18 to 27 GHz
Ka	27 to 40 GHz
V	40 to 75 GHz

Figure 5 Radio frequency bands [10].

ing number of satellites. In this section, 112 satellites providing total coverage were assumed. Afterwards the plots of the data rates over varying orbits, starting from LEO at 300 km all the way to GEO at 36000 km and their respective slant ranges are presented.

5.1 Radio Frequency

In the tables, the frequency bands are ordered from left to right from low to high frequency. Commonly used for satellite RF communication can be seen in Fig. 5. While typical bands used for small satellites are UHF, S, X, the move to higher frequency bands has been driven by a need for higher data rates [10]. Ku-, K-, and Ka-band communication systems are the state-of-the-art for large spacecraft, however, they are becoming more attractive for smaller sats due to the lower frequencies becoming more congested. For the scope of this paper, it was decided to include bands from S, X, Ku, Ka and V in order to show the development from low to high frequencies.

A standard conservative value for the noise Temperature of T_s = 290 K [16] and a standard value for other losses than the free-space loss, such as atmospheric attenuation and implementation losses of L = -9 dB [16] have been used for the computation.

The computations were conducted according to [16]. First, the equivalent isotropic radiated power was computed, which comprises the transmitter power P_t and gain G_t:

$$EIRP = P_t + G_t.[dB] \tag{1}$$

Next, the gain over noise temperature ratio:

$$G/T = G_a + G_r - 10 * log10(T_s), [dB/K] \tag{2}$$

where G_a and G_r are the antenna and receiver gain. As a third step, the free-space loss was calculated:

$$L_s = 20 * log10(4\pi R/\lambda)^2, [dB] \tag{3}$$

where R represents the orbital height and λ the wavelength. Now all these values combined result in the signal-to-noise ratio:

$$SNR = EIRP - L_s - L + G/T - k - 10 * log10(BW), [dB] \tag{4}$$

where k is the Boltzmann constant and BW is the bandwidth. Finally, using the Shannon-limit [17], the achievable data rate can be approximated:

$$DR = BW * log2(1 + SNR), [bps] \tag{5}$$

5.1.1 Downlink Budget

In Table 4 the results of the conducted downlink budget for RF communication at 600 km orbital altitude are summarized. As was to be expected, the lowest and highest data rates can be achieved with S-band at 0.9 Gbps and V-band at 57.4 Gbps, respectively. The fact that Ku-band data rates (7.3 Gbps) are below the equally high X-band (9.8 Gbps) and Ka-band rates (9.2 Gbps) might be surprising as one could assume that data rates will increase with frequency. This is not generally the case, as factors such as the BW play an important role too. The author of this paper decided to stick to commonly used values, supported by data sheets and other link budgets. Nevertheless, the choice of parameters can be easily adapted as desired. In order to get a better understanding of the data rate development over altitude and thereby distance between transmitter and receiver, the data rates have been plotted in Fig. 6. All frequency bands except for V-band show very similar development over altitude. It is interesting to see that for LEO altitudes the gap between V-band and the other bands is immense, however, the higher the orbit the lower the margin.

5.1.2 ISL Budget

In Table 5 the results of the ISL budgets for RF communication at 600 km orbital altitude, which corresponds to approximately 2720 km in slant range. The range between satellites was approximated by the distance between two adjacent satellites in a satellite constellation providing total coverage over the entire globe. Using the equations proposed in [11], the field of view of every satellite for an elevation angle of ten degrees, the radius of the spot size and the number of planes to

Table 4 RF communication downlink budget.

Link Budget - Downlink	S-band	X-band	Ku-band	Ka-band	V-band
Orbital height [km]	600				
Frequency [GHz]	3	8.2	15	28.5	40
BW [GHz]	0.05	0.375	0.750	0.5	4.5
EIRP [dBm]	28	48	40	68.4	28
G/T [dB/K]	34.4	44.9	12	13.6	49.4
SNR [dB]	55.44	78.46	29.32	55.51	38.4
Data rate [Gbps]	0.921	9.773	7.307	9.22	57.401

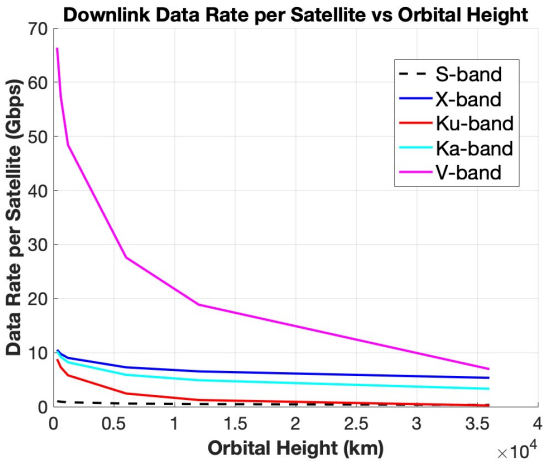

Figure 6 RF downlink data rate development over orbital altitude.

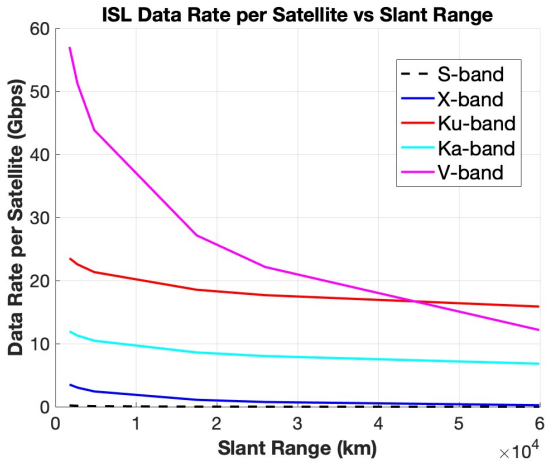

Figure 7 RF ISL data rate development over slant range.

cover all longitudes were calculated. From the amount of planes n_p, the angular separation between adjacent planes can be easily calculated to:

$$\vartheta = \pi / n_p . [rad] \tag{6}$$

Using basic geometry the following equation leads to the distance d:

$$d = 2 * alt * sin(\vartheta/2), [m] \tag{7}$$

in which case *alt* represents the sum of orbital altitude and the earth's radius. For ISLs, d shall be used instead of R for all equations introduced in Chapter 5.1. As will be pointed out later, the amount of satellites necessary to provide total coverage is considerably lower than the amount to satisfy the forecasted demand. In other words, the ranges included in these calculations represent maximum distances at the respective orbital altitudes, as the distances to be covered by signals are going to decrease with increasing number of satellites.

In similar manner to the downlink budget, S-band achieves the lowest and V-band the highest data rates at 0.1 Gbps and 51.2 Gbps, respectively. Data rates achievable with X-band (3 Gbps) are considerably lower than with Ka-band (11.3 Gbps), which on the other hand is about half of the Ku-band data rates (11.3 Gbps). Again, this is a matter of parameters that were chosen. The development of the data rates over slant ranges is represented in Fig. 7.

Except for V-band, all other bands show similar development over orbital altitude. In this case, V-band demonstrates a rather large margin to the other bands for low altitudes, however, towards GEO altitudes the data rates fall even below the ones achievable with Ku-band.

5.1.3 Direct-to-Device

Since direct-to-device (D2D) communication will certainly play an important role for a future space communication infrastructure, it was decided to also compute the link budget for the N256 S-band. It mainly differs in the frequency and BW, however, the size of the receiving antenna is a deciding factor. Considering the measurements of a common mobile phone as the ones currently in use, a built-in antenna will be around 10cm long. The results of the downlink budget are collected in Table 6, which are around 0.25 Gbps. The

Table 5 RF communication ISL budget.

Link Budget - ISL	S-band	X-band	Ku-band	Ka-band	V-band
Slant Range [km]	2720				
Frequency [GHz]	3	8.2	15	28.5	40
BW [GHz]	0.05	0.375	0.750	0.5	4.5
EIRP [dBm]	28	48	84	84	60
G/T [dB/K]	-0.6	12.9	51.4	32.5	35.4
SNR [dB]	8.31	24.33	90.57	67.91	34.27
Data rate [Gbps]	0.148	3.033	22.565	11.279	51.231

uplink data rates are expected to be higher due to a possibly larger receiving antenna. The data rate development over orbital altitude is shown in Fig. 8. The slope decreases strongly for low and more gradually for high altitudes.

Table 6 RF D2D downlink budget

.

Link Budget - Downlink	S-band (N256)
Orbital height [km]	600
Frequency [GHz]	2.2
BW [GHz]	0.01
EIRP [dBm]	28
G/T [dB/K]	13.62
SNR [dB]	27.12
Data rate [Gbps]	0.25

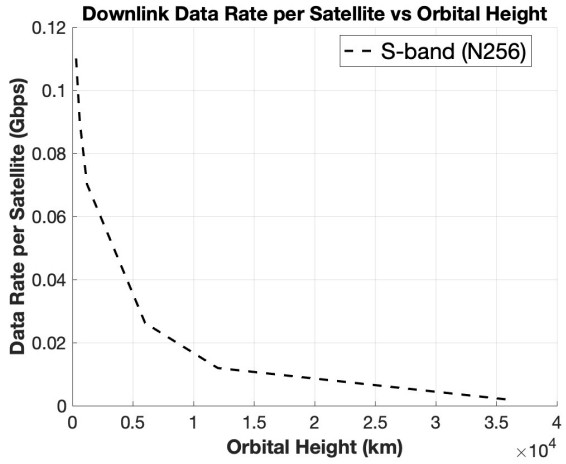

Figure 8 D2D downlink data rate development over orbital altitude.

5.2 Optical

The results of the optical link budget for downlink and ISL are collected in the tables below. For the computation, a standard conservative value for the noise Temperature of T_s = 290 K [16], a value for the beam divergence of θ = 0.001 in rad (for conservative approach the value in [18] was increased by one number of magnitude) and the atmospheric attenuation coefficient of α = 0.0002 in dB/m [19] have been used. Furthermore, the optical link budget was computed according to [18]:

$$P_r = P_t + 10 * log10(A_r) - 20 * log10(\theta * R) + exp(-\alpha * R), [dBW] \quad (8)$$

The received power P_r is computed with the transmitter power P_t, and the receiver area A_r. The slant range d was obtained in chapter 5.1.2. The free-space loss can be computed with:

$$F_s = 20 * log10(\lambda/4\pi R), [dB] \quad (9)$$

the SNR according to:

$$SNR = P_r - L_s - L - k - 10 * log10(BW), [dB] \quad (10)$$

where $G/T = G_t + G_r - 10 * log10(T_s)$. The achievable data rate can again be approximated by the Shannon-limit, as was shown in chapter 5.1.

5.2.1 Downlink Budget

In Table 7 the results of the conducted downlink budget for optical communication at 600 km orbital altitude are summarized . The data rates are around 8% percent

Table 7 FSO communication downlink budget.

Link Budget - FSO	Downlink
Orbital height [km]	600
Lambda [nm]	1545
BW [GHz]	1
Power received [dB]	-56.53
G/T [dB/K]	89.58
SNR [dB]	158.78
Data rate [Gbps]	52.744

lower than V-band downlink in RF communication and

considerably higher than the other bands, however, the chosen α is very low and can take values higher by orders of magnitude, depending on factors such as cloud coverage. Once again, the development over orbital altitude is plotted in Fig. 9. The slope shows similar features like V-band due to its steep slope for low orbits and gradual slope for higher orbits.

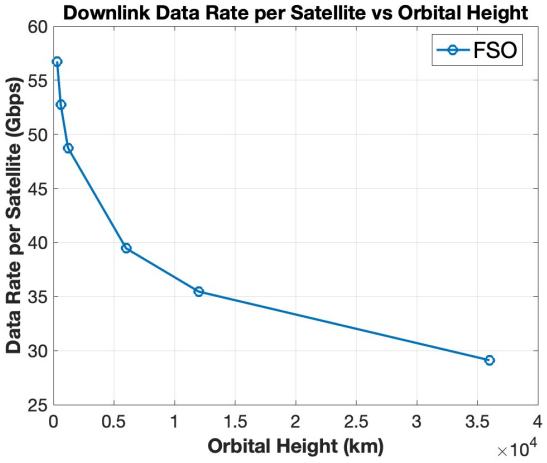

Figure 9 FSO downlink data rate development over orbital altitude.

5.2.2 ISL Budget

Now again, the values will be computed using the slant range d instead of the orbital height R. The results for the link budget at 600 km altitude corresponding to 2720 km slant range are collected in Table 8. The

Table 8 FSO communication ISL budget.

Link Budget - FSO	ISL
Slant Range [km]	2720
Lambda [nm]	1545
BW [GHz]	1
Power received [dB]	-69.66
G/T [dB/K]	151.64
SNR [dB]	218.21
Data rate [Gbps]	72.488

data rates for ISL are generally higher than the ones for downlink due to no atmospheric attenuation, however, the features of the slope are very similar. The data rates are 41% higher than V-band ISL, showing the huge advantage of FSO communication for ISLs. In addition, the margin will most likely increase even further due to decreasing distances between satellites with increasing total number of satellites as was explained in chapter 5.1.2 . Graph Fig. 10 is showing the development of the data rates over increasing slant ranges.

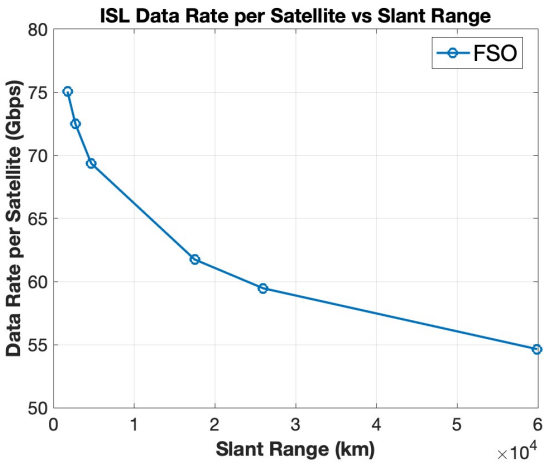

Figure 10 FSO ISL data rate development over orbital altitude.

5.3 Discussion

All slopes have similar traits, the achievable data rates decrease with increasing distance to the receiver, as was to be expected due to the signal strength's dependency on distance. The slopes for downlink decrease generally faster than ISLs, with V-band having the largest gradients, ahead of optical links. All other frequency bands show a very similar slope only shifted in y-direction. At an orbit of 600 km, the highest data rates can be achieved with optical ISLs at 72.5 Gbps, followed by V-band downlink at approximately 57.4 Gbps. Optical downlink and V-band ISL are only around 10% lower with 52.7 Gbps and 51.2 Gbps, respectively. All other frequency bands are considerably lower, with S-band achieving the lowest data rates, 0.9 Gbps for downlink and 0.1 Gbps for ISLs, representing around 1% and less. Further analysis ensured that the receiving antennas stay within certain diameter limits. Ground station antennas were kept below a 6 m radius, satellite antennas below 0.5 m, and device antennas below 0.1 m. The equations used [16] to compute the effective aperture are:

$$A_{eff} = G * \lambda^2/(4\pi A), [m] \tag{11}$$

where G is the linear gain, c is the speed of light, and A is the receiving area. With A_{eff} the receiving antenna diameter can be computed according to:

$$D = \sqrt{(x/\pi)}, [m] \tag{12}$$

The results for the optical link budget seem high in comparison to the ones in [18], however, other parameters were chosen and due to the conceptual state available literature is limited. It should not be neglected that these values will change considerably when changing parameters. It is also important to mention that for simplicity no modulation or coding schemes, no compression techniques and no other forms of communication were considered, which will also have a considerable influence on the final results. Additionally, another assumption of the model is that the human technological competence will not advance and remain at the same level at which it is right now. Lastly, in terms of the model, all types of communication have been implemented, however, the model only considers RF communication downlink for the further computations. Reasons for this are that downlink data rates are the bottleneck of a space-based communication infrastructure, and due to the high influence of weather attenuation, optical communication is not suitable for downlinks. Furthermore, optical communication clearly has advantages for ISLs, however, at the moment it is still conceptual and not commercially used. Nevertheless, it is being tested and since it has already been implemented, it can easily be connected to the model in the future.

6 Results

In this part of the paper, the results of the model will be analyzed, discussed and evaluated. Furthermore, validation of the model with its results will be achieved by comparison to Starlink, SpaceX's space-based communication infrastructure.

6.1 Forecast Model

The process is shown according to the following examples. In order to estimate the global internet users, the penetration depth was computed with the estimated global population for each year [20] and statistical data on the global internet users from [7] between 2005 to 2023. The development of the penetration depth was then estimated making use of the sigmoid function, which is a logistic function approaching full internet penetration. The results can be seen in Fig. 11, which shows that the entire global population will be connected to the internet no later than 2060. The current increase is also in accordance with the data collected in [21], which shows exponential growth of the internet penetration depth of the least developed and developing countries, while developed countries exhibit continuous linear growth in the current time.

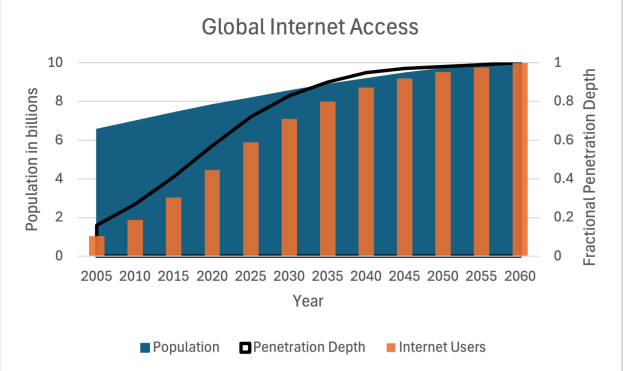

Figure 11 Global internet access forecast.

Table 9 shows the results of the demand model for the category "global internet users" until 2060. As already mentioned before, the population will continuously grow from around 8 billion in 2024 to almost 10 billion in 2060. While before 2020, only half of the global population had internet access, it is shown that according to the forecast the entire global population is expected to be connected until 2060. Finally, the peak global users were obtained by assuming that within a workday period of 14 hours, the entire eastern hemisphere could be accessing the internet simultaneously, representing a maximum of 7/8 of the population as can be seen in Fig. 12. While people in Western Europe are starting their day, the ones in Eastern Russia and Australia are ending theirs.

This assumption will most likely not prevail, since especially the population on the Asian and African continent is expected to grow in a considerably higher pace than other populations [22], leading to an increase in peak global users over time.

Table 10 displays the results of the forecast considering the category "devices". A linear growth of devices per capita and IoT devices can be seen, which also represents other forecasts found online [23], [24]. In 2020 every human had on average 2.7 devices connected to the internet. While North America and Western Europe had a considerably higher count between seven and ten, the other parts of the world lowered the average, ranging only from a little over one to 3.5 [25]. Nevertheless, the overall average number will increase to almost ten in 2050. Furthermore, it is shown that the share of IoT devices increases in comparison to overall devices. While in 2020 it was approximately half, in 2050 the share amounts to almost 60%.

The forecast results for "data rates" can be found in Table 11. While the average BW per smartphone

Table 9 Model output for Global Internet Users.

Forecast	Global Internet Users			
Year	Population [billions]	Internet Users [billions]	Penetration Depth (computed) [%]	Peak Global Users [billions]
2005	6.56	1.023	15.59	-
2010	6.99	1.981	28.34	-
2015	7.43	2.954	39.76	-
2020	7.84	4.585	58.48	4.012
2025	8.19	5.9	72	5.163
2030	8.55	7.1	83.04	6.213
2035	8.88	7.992	90	6.993
2040	9.19	8.731	92.2	7.64
2045	9.47	9.186	97	8.038
2050	9.71	9.516	98	8.327
2055	9.85	9.752	99.01	8.533
2060	*9.99*	*9.99*	*100*	*8.741*

Table 10 Model output for Devices.

Forecast	Devices			
Year	Devices per Capita	Total Connected Devices (IoT) [billions]	Total Connected Devices (overall)[billions]	Peak Connected Devices [billions]
2015	-	3.6	-	-
2020	2.7	11.3	21.2	18.6
2025	4.0	18.7	32.8	28.7
2030	5.1	26.4	43.6	38.2
2035	6.3	34.1	55.9	49
2040	7.5	41.8	68.9	60.3
2045	8.7	49.5	82.4	72.1
2050	9.9	57.2	96.1	84.15

in 2020 was a little under 2 GB/moth [26], it will increase exponentially up to 342 GB/month in 2050. An even steeper increase shows the global BW, which will grow by a factor of almost 35 until 2050. The listed use cases [27], [28] assume that only 1% of the peak global users are conducting said activity. It leaves room to play around with different scenarios to fulfill the Global BW forecast. In reality, there will be thousands of use cases, as very rarely a user fits in only one of the cases, but rather conducts a mixture of use cases. An example is social media, as it comprises watching high-definition videos and photos, messaging and reading articles. In 2020, the global BW amounted to 719 Tbps [29], but the network capacity is set to increase to almost 25 Pbps in 2050.

6.2 Architecture model

For the architecture model, it is assumed that the entire global data traffic is handled by a space-based infrastructure. The scatter plot Fig. 13 shows the total number of satellites required to provide a certain data rate per user, while also providing information on the total possible user coverage for every configuration. Pointing out that every fourth configuration represents the same frequency, one can clearly rule out S-band as a feasible configuration. Not only requires it a drastically higher amount of satellites, the number is in fact so high that it lies in the range of the other bands providing a data rate per user which is higher by an order of magnitude. To give an example, this can be seen in configuration 1 with the first blue dot on the left-hand side of the plot. For an orbital altitude of 300 km and 30° inclination around 3040 satellites using S-band are required to provide 1 kbps/user. At the same altitude and inclination 2950 satellites for X-band (configura-

Table 11 Model output for Data Rates.

Forecast	Data Rates					
Year	Per Smartphone [kbps]	Peak BW for Use Cases [Tbps]				Global BW [Tbps]
		Online calls (0.5 Mbps)	Instant Messaging (1 Mbps)	Online gaming (4 Mbps)	4K Streaming (25 Mbps)	
2020	7.6	-	-	-	-	719
2025	12	29	57	229	1433	2270
2030	25	37	75	299	1870	4791
2035	44	39	78	311	1943	8301
2040	68	40	80	322	2010	12800
2045	97	41	83	332	2072	18288
2050	132	42	85	340	2124	24765

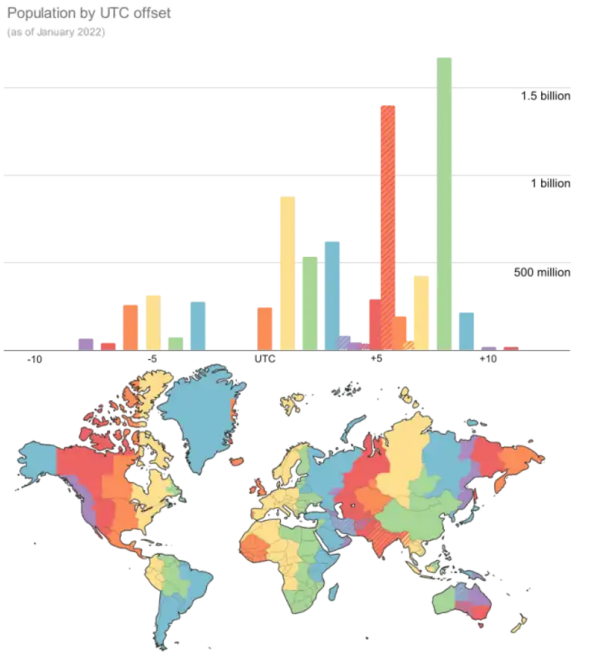

Figure 12 World map showing the population distribution per time zone [20].

tion 2, red dot), 3524 for Ku (configuration 3, red dot) and 3037 for Ka-band (configuration 4, red dot) would be required to provide 10 kbps/user.

Therefore, and for better visibility, the graph Fig. 14 has been reduced to the relevant configurations and due to the similarity in patterns zoomed in, only showing the data points for 1 kbps/user. As can be seen now, the number of satellites required increases with the orbital altitude as well as inclination. When comparing configurations 2 and 18, the number of satellites increases from around 295 to 318, stating that the orbital altitude has only a minor effect. When comparing configurations 2 and 6, the number increases from 295 to 443, showing that a change in inclination leads to a drastic increase. This is due to the rising percentage of users served with increasing inclination. Finally, it can be said that the most efficient configurations make use of X-band communication and low inclinations.

Since the orbital altitude barely impacts the number of satellites the choice is rather arbitrary. While lower altitudes minimize latency, the atmospheric drag increases significantly, impacting satellite lifespan and necessitating propulsion systems for orbit-raising maneuvers. On the one hand a higher orbit experiences less drag, however, on the other hand launch costs are increased due to larger fuel requirements and a smaller payload. The orbital altitude of 600 km is therefore chosen as the ideal match. Furthermore, another trade-off needs to be conducted between providing total global coverage with a high number of satellites or serving a large portion of users with a considerably fewer satellites. Due to the objective of providing global coverage, 90° is chosen as an ideal configuration, covering all of the global population on all parts of the globe. In summary, configurations featuring 600 km altitude, X-band, and inclinations around 90° offer a feasible balance of satellite count and coverage, aligning well with the goal of high-population coverage while minimizing infrastructure complexity. The ideal solution in terms of coverage and satellite count will likely be a combination of orbits of different inclinations, just as SpaceX has done with Starlink, which could be considered in future works. The results are summarized in the Table 12.

Finally, for the matter of scalability, the final number of satellites mainly depends on the BW per user that should be provided. In the following graph the development of the number of satellites is shown in relation to increasing data rates in kbps. If every user should be provided with a BW of 10 kbps, at 600 km using X-band 3176 satellites are required for 30° inclination, 4763 for 45°, 6033 for 60° and 6351 for 90°.

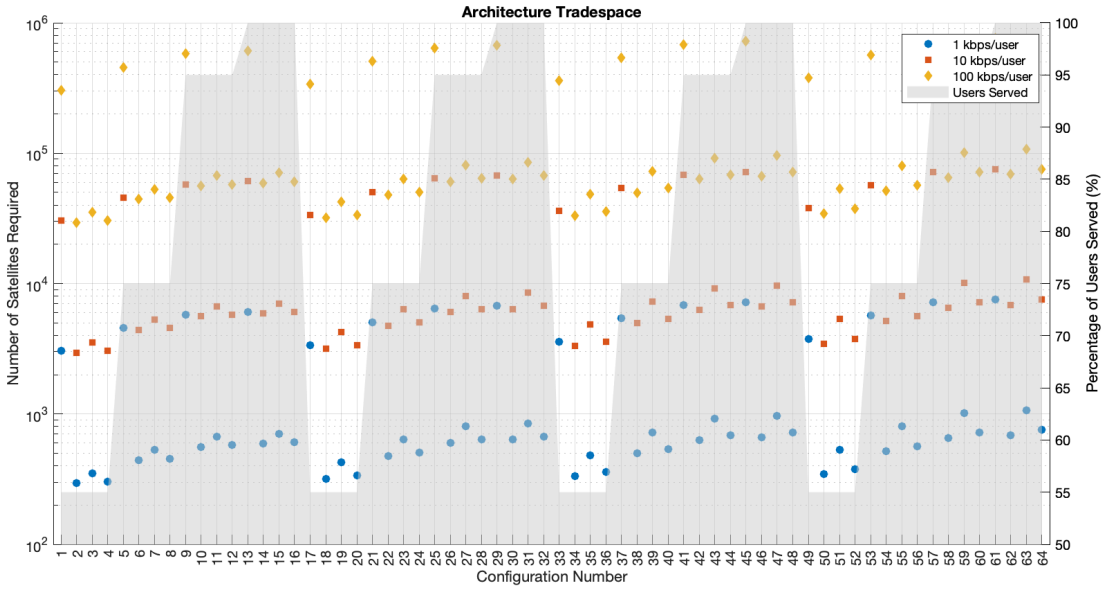

Figure 13 Number of satellites and percentage of users served for all architecture configurations.

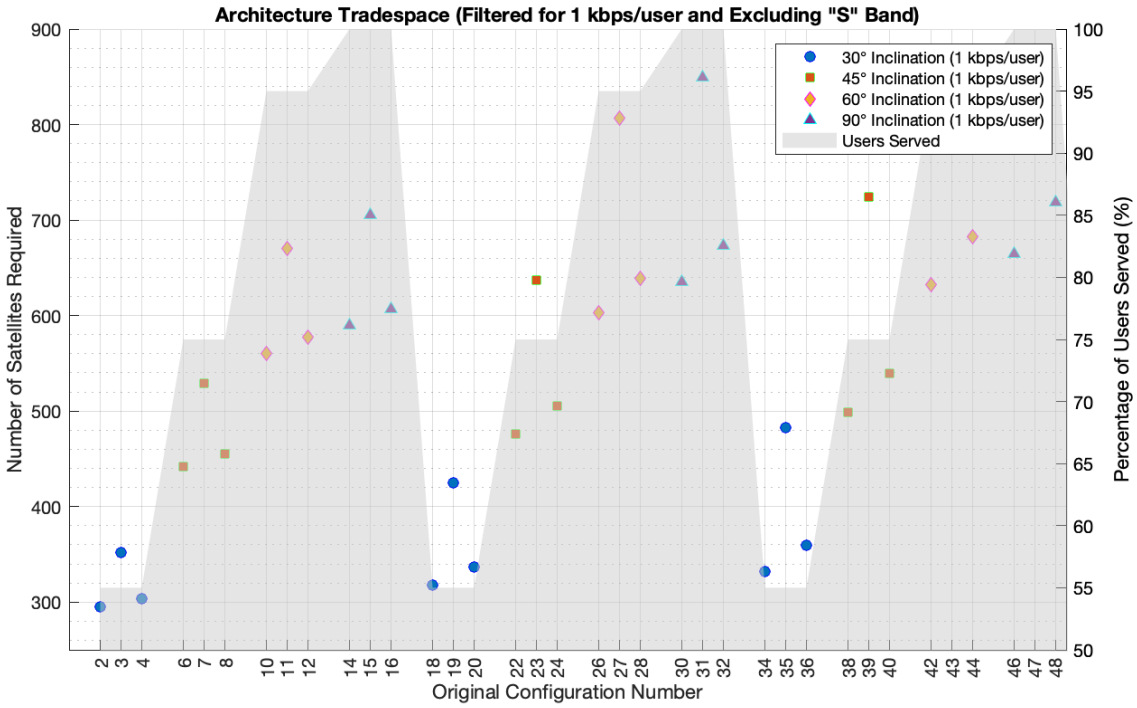

Figure 14 Number of satellites and percentage of users served for the relevant architecture configurations.

In conclusion, configurations with higher inclinations offer broader geographic coverage but typically require more satellites, especially in high-density population areas. For instance, an inclination of 90° enables global coverage but may necessitate up to twice as many satellites compared to configurations with inclinations of 30°. Additionally, while the orbital altitude does not have a big influence on the satellite count, it can greatly effect launch and/or operating costs of such a constellation. Table 13 provides an overview of the required X-band satellites for different data rates at 600 km orbital altitude.

As a next step, the architectural model has been provided with decided on variables, namely the year

Table 12 Best choice of architectures providing 1 kbps/user at different population coverages.

Altitude [km]	**Inclination** [°]	**Band**	**Satellite Count**	**Coverage** [%]
600	30	X	318	55
600	45	X	477	75
600	60	X	604	95
600	90	X	636	100

Table 13 Number of X-band satellites required to achieve certain data rates with different inclinations at 600km.

Inclination [°]	**1 kbps/user**	**10 kbps/user**	**100 kbps/user**	**1 Mbps/user**
30	318	3176	31751	317508
45	477	4763	47621	476210
60	604	6033	60330	603295
90	636	6351	63502	635015

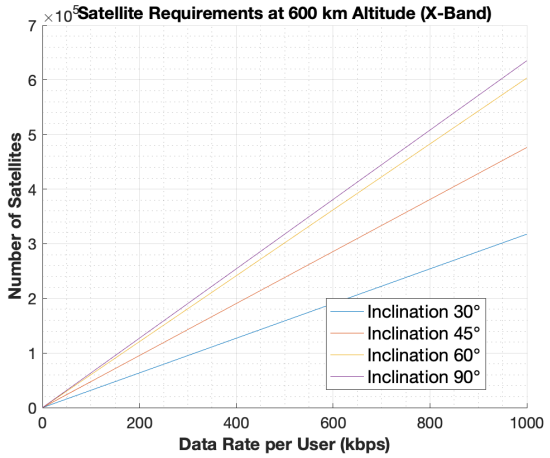

Figure 15 Number of X-band satellites at 600 km over data rate per user for different inclinations.

2030, 600 km orbital height above the surface and 90° inclination for global coverage. The most important results are collected in Table 14, and for completeness the results have been collected for all the previously discussed frequency bands. The global BW and data rates per satellite have already been discussed in the link budget (chapter 5). The BW per user is shown one time for the global peak user, and one time for the population density of Asia, which is 155 people/km^2 [30], as it is the highest density in the world and will represent another limit case. The proposed architecture will result in every configuration in 28 kbps per user for Asia and in 641 kbps for the global peak. Through downlink from one satellite to one ground station only, around 80 Tb for S-band and up to almost 5 Pb for V-band can be transferred every day. The other bands range from 0.6 to 0.84 Pb/day. Considering downlink from a satellite to a user, in Asia each user would receive a daily transferable data rate of almost 2.5 Gb/day, and the average for peak global users would amount to over 5.5 Gb/day, which is more than double. As was to be expected, with rising data rates per satellite, the minimum number of satellites required to cover the demand will decrease. This number ranges from 5.2 million satellites for S-band frequency to 83 thousand satellites for V-band, however, for the other bands the average is around 550 thousand satellites. For comparison, the minimum amount of satellites to provide total coverage at this orbital altitude amounts to only 112. Every satellite configuration leads to a different constellation, ranging from under 3951 planes with 1317 satellites each to 500 planes with 166 satellites each, for S and V-band respectively. Due to the sheer amount of satellites in the same orbit and because of that, very short distances , the one-way latency for ISLs amounts to 3.7e-3 ms for S-band and 0.3 ms for V-band, for the other bands the signal takes a little over 0.1 ms. For downlink the latency equals 2 ms. In order to put in perspective how many users per satellite every constellation could serve, the global peak users as well as the population density in Asia were considered. While the global peak users per satellite are between 1.4 and 90 thousand, in Asia the number lies between 32.5 thousand and over two million.

6.3 Final Model

As the final step, the overall architecture model is run in iterations against technological constraints, while the input remains the same. These launch-imposed constraints consider predicted launch capabilities and capacities, which are investigating if the proposed architecture is feasible. They are defined as follows: according to statistics [31] the average annual growth rate of space launches between 2008 and 2018 was 4.18%,

Table 14 Summary of the architecture proposals projected for the year 2030 at 600 km altitude and 90° inclination.

Results			S-Band	X-Band	Ku-band	Ka-band	V-band
Network Capacity	Global BW (Tbps)		4791				
	Data rate per Satellite [Gbps]		0.921	9.773	7.307	9.22	57.401
	BW per User [kbps]	Asia	60.61				
		Global Peak	77.2				
	Daily transferable data rate	Per GS [Tb/day]	79.6	844.4	631.3	796.6	4959.4
		Per Device [Gb/day]	2.448 (Asia); 5.534 (Global Peak)				
Proposed Constellation	Min Number of Satellites [thousands]	Cover Demand	5203	490.2	655.7	519.6	83
		Total Coverage	112				
	Number of Planes		3951	1214	1402	1250	500
	Satellites per Plane		1317	404	468	416	166
	Latency (one-way) [ms]	Downlink	2				
		ISL	0.0037	0.12	0.1	0.12	0.29
User Configuration	Users per Satellite [thousands]	Asia	15.19	161.3	120.6	152.1	947.1
		Global Peak	11.93	126.6	94.65	119.4	743.5

however, in the following five years the growth rate increased to an average of 16.77% with 223 launches in 2023. Assuming exponential growth at this rate from here on, the yearly amount of launches in the future can be estimated:

$$launches = 223 * 1.1677^{year-2023},$$

Together with the number of satellites that can be launched at a time and their lifetime, the satellite population can be computed.

$$population = launches * satellites * lifetime,$$

The loop checks if the achievable satellite population for satellite lifetimes of five, seven and ten years, equals or surpasses the minimum required number of satellites for at least one of the configurations. If this is not the case, the demand is reduced by 5% and the model is run another time, until at least one configuration meets the constraints. To give an example, if the model is run iteratively with a capacity of 15 satellites per launch the following output will result: For a lifetime of five years a total satellite population of just under 50 thousand would be in orbit, which would allow a V-band configuration to satisfy around 57%. With a lifetime of seven years and almost 70 thousand satellites in orbit, more than 80% of the initial demand could be covered and for a lifetime of ten years almost 100 thousand satellites in orbit could account for 100% of the estimated demand using V-band. Changing the value of satellites per launch to 60 as was done by SpaceX [32] numerous times, all satellite lifetimes would lead to V-band populations large enough to account for the entire demand. However, as stated before V-band is not a feasible communication band for downlink and still no other configuration would be feasible, as an X-band configuration would require the second lowest population of 490 thousand but even with a lifespan of ten years, less than 400 thousand satellites would be in orbit. In order to cover the full demand also for other configurations, one of the three parameters must be increased. As satellites are becoming more and more compact, and with large launchers like Starship by SpaceX, the variable most likely and most feasible to increase is the launch capacity. Table 15 displays the launch capacity required for every band and lifespan in order for the infrastructure to be able to satisfy 100% of the demand. While the capacity required for V-band is already achievable and has been demonstrated, X-band and Ka-band already require more than 75 satellites per launch for a lifetime of 10 years. This implies the need for further size and mass reductions in order to make this feasible. To further support the previously made decision on frequency bands, S-band requires almost 800 satellites per launch with a ten year lifespan, which makes this configuration impossible to implement without increasing both launches and lifetime. Lastly, a simple sensitivity analysis was conducted, examining the impact of possible launch failures and non-functional satellites on the overall system performance in terms of BW. It was shown that, in general, launch failures lead to a higher percentage of non-functional satellites than hardware malfunctions within the satellite, and therefore have a bigger impact on system performance.

6.4 Validation

Firstly, in order to validate the correctness and functionality of the model, the general output has been

Table 15 Solution for increased launch capacity in 2030.

Frequency band	Number of Satellites required [thousands]	Satellites required per Launch per Lifetime			Demand reduction [%]
		5 years	7 years	10 years	
S-Band	5203	1577	1126	789	0
X-Band	490	149	107	75	0
Ku-band	656	199	142	100	0
Ka-band	520	158	113	79	0
V-band	83	26	19	13	0

analyzed. As can be seen in Fig. 16, the forecast expects the global demand to increase exponentially over the next decades, as it is expected by many analyses online. Related to an increase in BW is the number of satellites required, which is nicely shown. The expected gap between S-band and other bands can be clearly seen, and the distribution of the other bands represents the results from the link budget.

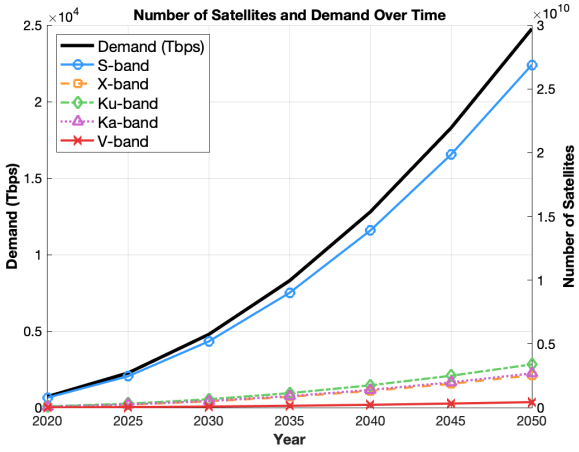

Figure 16 Demand and number of satellites required over time.

Fig. 17 is showing the number of satellites for the bands and its influence on latency for ISL. The higher the number of satellites in orbit, the shorter the distances a signal must traverse for a successful link, resulting in a shorter time, and vice versa. This represents reality and is therefore a proof of theoretical correctness. Now, in order to validate the model's technical output and ensure its credibility, the work done in [12] is being used to compare and check the results of this paper. The focus lies on SpaceX's Starlink, which was analyzed among other satellite constellations. 4425 satellites are considered to be in orbit, allowing a maximal total system throughput of 23.7 Tbps. This translates to an average of 5.4 Gbps and a maximum of 21.4 Gbps per satellite, achieved by a

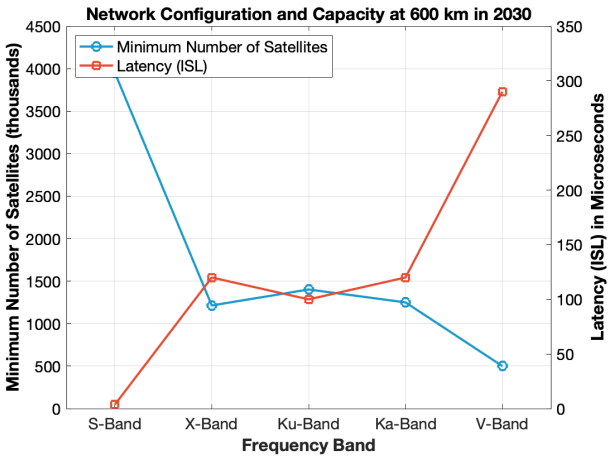

Figure 17 Minimum number of satellites and latency for ISL over frequency.

Ku-band and Ka-band constellation at orbital altitudes between 1110 and 1325 km. The average values computed by the model for an average altitude of 1200 km are 7 Gbps, representing values in a similar range, yet almost 30% higher. It should not be neglected, that for the scope of this paper the link budget conducted is rather basic and does not consider coding and modulation schemes. Error-correcting codes improve reliability but may reduce data rates due to added bits. Modulation, on the other hand, can increase data rate by transmitting more bits per symbol, however, it requires an improved signal quality to avoid errors which reduces reliability. A trade-off always needs to be conducted. While Starlink is currently promising a download user BW of 25 up to 220 Mbps [33], this is mostly due to comparably low subscriber count, which just surpassed 4 million [34]. For comparison, the predicted number for internet users is more than one thousand times higher, at around 4.5 billion. This amount of active users would lower the BW available to every user by the same factor, which puts it within the range of the model's output of tens of kbps. Moving on from the results for network capacity to the proposed

constellation, the physical asset is considered. Since the number of satellites is depending on the data rate per satellite, it is not surprising that the model's values are also 26% lower than the number of satellites that would be required with Starlink satellites. Similarly, other results related to the constellation are computed based on these values. Finally, there are 6400 currently active Starlink satellites in orbit [35], however this number keeps increasing so no validation on the user configuration can be made. Nevertheless, as other important model outputs have been validated, the credibility and theoretical righteousness of the model have been proven.

6.5 Future Work and Outlook

Finally, an outlook on further work and development on this topic is given. While the overall topic is still mainly theoretical, some players such as SpaceX are attempting to build a space-based communication architecture. Unfortunately, these companies keep most of their data confidential which shows the importance of this work, leading to a better understanding of the requirements and challenges that have to be accounted for in order to undertake such a project on a global scale. As next steps, the complexity of every aspect of the model can be further increased. Starting with the communication section, the link budgets should be enhanced, including coding and modulation to obtain more precise results closer to reality. Furthermore, estimations on the development of data handling should be made, taking into account techniques such as data compression to provide a more realistic approach to the architecture proposal. As of now, only RF downlink communication has been connected to the model, however, other link budgets have been implemented as well and can be used for different scenarios or other possible use cases, especially optical communication. Another step would be to not only examine single types of orbits only different in RAAN for the entire constellation, but rather a mixture of inclined orbits, just like Starlink is doing. Assuming ISL, this will likely result in a reduced satellite population [11]. Additionally, the boundary conditions of this topic should be extended, not only considering the communication network, but the entire data traffic that needs to be transported by an infrastructure, including navigation, earth and deep-space observation. What should be done, as well, is a detailed sensitivity analysis, considering what would happen in case of a catastrophe, both man-made such as a chain reaction or of natural cause such as a severe solar storm. This could possibly be done in parallel with further optimizing the architecture, making use of techniques such as uncertainty modeling. Finally, while the proposed architecture theoretically meet technical and cost objectives, its sustainability hinges on addressing risks like orbital debris. Future models should incorporate mitigation strategies to ensure the feasibility of long-term satellite operations. In conclusion, the next steps are:

- Revise link budgets and increase complexity
- Introduce simulations incorporating mixed-inclination orbits
- Evaluate the economic and technical feasibility of implementing optical ISLs in future constellations
- Assess the impact of orbital debris on long-term sustainability

7 Conclusion

In conclusion, the research questions will be answered.

- **How can a predictive demand model be used to design a scalable, space-based communication infrastructure that meets the future requirements of global coverage and connectivity?**

  While it is comparably straight-forward to predict the global internet users in the future, the development of other aspects such as data rates are not as clearly defined, since technological advancements are impossible to predict but can have a huge impact on the outcome. Using predicted values such as global BW, the simulations propose feasible space-based architectures to meet this demand. A key finding is that doubling the data rate per user requires doubling the number of satellites, demonstrating the system's scalability. Additionally, increasing the inclination of X-band satellites from 30° to 90° doubles the number of satellites required, while doubling the orbital altitude raises the requirement by about 8%. However, the sheer number of satellites required to meet the predicted demand in 2030 is extremely high. This raises concerns about the feasibility of launching, operating, and maintaining such a vast infrastructure, as well as the potential for increased orbital congestion.

- **Which space-based architecture maximizes coverage while minimizing costs?**

The decision variables in the architecture design include orbital altitude, inclination, and the frequency band used for communication. Among these, X-band proved to be the most effective option with current technology. X-band requires, on average, 94% of the satellites needed for Ka-band, 74% of Ku-band, and less than 10% of S-band. Additionally, selecting X-band at a 90° inclination and 600 km orbital altitude was shown to maximize global coverage while minimizing operational and setup costs. These findings indicate that X-band is the optimal choice under current conditions, balancing coverage and costs effectively.

- **How can such an infrastructure be implemented, considering technical and launch constraints required to ensure its feasibility?**

  To determine the technical feasibility of the proposed architecture, launch constraints and capacities were analyzed. For the predicted demand in 2030, a launch capacity of 75 satellites per launch with an annual launch rate of 661 and a ten-year satellite lifetime is necessary. For Ka-band, the required launch capacity increases by 5%, for Ku-band by 33%, and for S-band, it increases more than tenfold. V-band offers a potentially viable alternative, requiring 83,000 satellites at 600 km to meet the demand—an order of magnitude closer to SpaceX's planned population of over 40,000 satellites. However, V-band faces challenges with downlink communication due to atmospheric attenuation and scintillation effects [36]. While the launch capacity for X-band is already in reach, as demonstrated by SpaceX's capability to launch up to 60 satellites at once even before Starship [32], the launch rate must be increased three fold to meet the requirements. Lowering the satellite lifetime by half would also require doubling either the launch capacity or the launch rate, or increase both with a combination of factors. Despite these technical capabilities, concerns about the sustainability of such a large satellite population arise, particularly regarding the risk of Kessler syndrome, where colliding debris leads to cascading collisions [37]. Finally, the foundational assumption that the entire global BW must be handled by space-based downlink communication underscores the importance of integrating ground infrastructure to make the system technically feasible and functional. A hybrid approach combining space- and ground-based architectures could mitigate risks and enhance system reliability.

References

[1] Ericsson. Mobile traffic forecast, 2024. URL https://www.ericsson.com/en/reports-and-papers/mobility-report/dataforecasts/mobile-traffic-forecast. Accessed: August 2024.

[2] SpaceX. Starlink. https://www.starlink.com, 2024. Accessed: 2024-07-25.

[3] OneWeb. Oneweb. https://oneweb.net, 2024. Accessed: 2024-07-25.

[4] Mohammmadnour Mosbah Aljarrah, Farah H. Zawaideh, Murad Magableh, Hassan Al Wahshat, Rajina R. Mohamed, and Archana K V. Internet of thing (iot) and data analytics with challenges and future applications. In *2023 International Conference on Computer Science and Emerging Technologies (CSET)*, pages 1–8, 2023. doi: 10.1109/CSET58993.2023.10346664.

[5] Tejendra Rathod, Niket Kumar Jadav, Sudeep Tanwar, Zdzisław Polkowski, Naveen Yamsani, Reetika Sharma, Fares Alqahtani, and Ahmed Gafar. Ai and blockchain-based secure data dissemination architecture for iot-enabled critical infrastructure. *Sensors*, 23(21):8928, 2023. doi: 10.3390/s23218928. URL https://www.mdpi.com/1424-8220/23/21/8928.

[6] Janet Abbate. *Inventing the Internet*. MIT Press, Cambridge, MA, 1999.

[7] Statista. Number of internet users worldwide, 2024. URL https://www.statista.com/statistics/273018/number-of-internet-users-worldwide/. Accessed: June 17, 2024.

[8] Yuchnovicz Gheorghe, A.V. The space infrastructure vulnerability cadastre: Orbital debris critical loads. *Int J Disaster Risk Sci 6, 359–371*, 2015.

[9] Naveed UL Hassan, Chongwen Huang, Chau Yuen, Ayaz Ahmad, and Yan Zhang. Dense small satellite networks for modern terrestrial communication systems: Benefits, infrastructure, and technologies, 2020. URL https://arxiv.org/abs/2007.15377.

[10] NASA, Feb 12, 2024. URL https://www.nasa.gov/smallsat-institute/sst-soa/soa-communications/. Last accessed 5 September 2024.

[11] Troy D. Rockwood, Moriba K. Jah, and Yang Cheng. *Optimization of Inter-Constellation Data Transport Using a Satellite Ring*. aerospace research central, 4 Jan 2024. doi: 10.2514/6.2024-2280. URL https://arc.aiaa.org/doi/abs/10.2514/6.2024-2280.

[12] Inigo del Portillo, Bruce G. Cameron, and Edward F. Crawley. A technical comparison of three low earth orbit satellite constellation systems to provide global broadband. *Acta Astronautica*, 159:123–135, 2019. ISSN 0094-5765. doi: https://doi.org/10.1016/j.actaastro.2019.03.040. URL https://www.sciencedirect.com/science/article/pii/S0094576518320368.

[13] Visual Capitalist. Mapped: The world's population density by latitude, 2024. URL https://www.visualcapitalist.com/cp/mapped-the-worlds-population-density-by-latitude/. Accessed: October 2024.

[14] Pierre Bernhard, Marc Deschamps, and Georges Zaccour. Large satellite constellations and space debris: Exploratory analysis of strategic management of the space commons. *European Journal of Operational Research*, 304(3):1140–1157, 2023. ISSN 0377-2217. doi: 10.1016/j.ejor.2022.04.030. URL https://doi.org/10.1016/j.ejor.2022.04.030.

[15] Kongsberg Satellite Services (KSAT). Ksat white paper: Ka-band and the future of big data from space. https://www.ksat.no/globalassets/ksat/documents/ksat_white_paper.pdf, 2023. Accessed: 2024-07-25.

[16] Otto Koudelka. Link budget calculations. ITU. URL https://www.itu.int/en/ITU-R/space/workshops/2015-prague-small-sat/Presentations/ITU-linkbudget.pdf.

[17] James R. Wertz and Wiley J. Larson. *Space Mission Analysis and Design*. Kluwer Academic Publishers, Dordrecht, The Netherlands, 3rd edition, 1991.

[18] Dirk Giggenbach, Marcus T. Knopp, and Christian Fuchs. Link budget calculation in optical leo satellite downlinks with on/off-keying and large signal divergence: A simplified methodology. *International Journal of Satellite Communications and Networking*, 41(5):460–476, 2023. doi: https://doi.org/10.1002/sat.1478. URL https://onlinelibrary.wiley.com/doi/abs/10.1002/sat.1478.

[19] Nadav Levanon. Radar. In Robert A. Meyers, editor, *Encyclopedia of Physical Science and Technology (Third Edition)*, pages 497–510. Academic Press, New York, third edition edition, 2003. ISBN 978-0-12-227410-7. doi: https://doi.org/10.1016/B0-12-227410-5/00973-X. URL https://www.sciencedirect.com/science/article/pii/B012227410500973X.

[20] Gaël de Mondragon, January 13, 2022. URL https://distributionofthings.com/world-population-by-time-zone/. Last accessed 10 July 2024.

[21] Statista. Share of internet users worldwide by market maturity, 2024. URL https://www.statista.com/statistics/209096/share-of-internet-users-worldwide-by-market-maturity/. Accessed: June 17, 2024.

[22] INED. World population projections by continent, 2024. URL https://www.ined.fr/en/everything_about_population/data/world-projections/projections-by-continent/. Accessed: September 12, 2024.

[23] Statista. Iot connected devices worldwide, 2024. URL https://www.statista.com/statistics/1183457/iot-connected-devices-worldwide/. Accessed: June 17, 2024.

[24] Transforma Insights. Forecast highlights, 2024. URL https://transformainsights.com/research/forecast/highlights. Accessed: June 17, 2024.

[25] Statista. Global number of devices and connections per capita 2018-2023, 2024. URL https://www.statista.com/statistics/1190270/number-of-devices-and-connections-per-person-worldwide/. Accessed: June 17, 2024.

[26] Statista. Worldwide monthly data traffic per smartphone, 2024. URL https://www.statista.com/statistics/738977/worldwide-monthly-data-traffic-per-smartphone/. Accessed: June 17, 2024.

[27] VdoCipher. Video bandwidth explanation, 2024. URL https://www.vdocipher.com/blog/video-bandwidth-explanation. Accessed: August 2024.

[28] G. Vargas Avila, M. Anastasopoulos, Z. Liao, et al. System design study of a constellation of small spacecraft to deliver seamless 5g connectivity to unmodified cell phones through an end-to-end non-terrestrial network. In *74th International Astronautical Congress (IAC) 2023*, Baku, Azerbaijan, October 2-6 2023. Paper number 77798.

[29] International Telecommunication Union (ITU). International bandwidth usage, 2022. URL https://www.itu.int/itu-d/reports/statistics/2022/11/24/ff22-international-bandwidth-usage/. Accessed: June 17, 2024.

[30] Worldometer. Asia population, 2024. URL https://www.worldometers.info/world-population/asia-population/#:~:text=Asia%20population%20is%20equivalent%20to,401%20people%20per%20mi2). Accessed: July 17, 2024.

[31] Günter's Space Page. Launch schedule 2024, 2024. URL https://space.skyrocket.de/doc_chr/lau2024.htm. Accessed: September 11, 2024.

[32] Spaceflight Now. Spacex successfully deploys 60 more starlink satellites, but loses booster on descent, 2021. URL https://spaceflightnow.com/2021/02/16/spacex-successfully-deploys-60-more-starlink-satellites-but-loses-booster-on-descent/. Accessed: September 12, 2024.

[33] Starlink. Starlink legal document: Doc-1400-28829-70. URL https://www.starlink.com/legal/documents/DOC-1400-28829-70. Accessed: 2024-11-17.

[34] TechCrunch. Starlink will hit 4 million subscribers this week, spacex president says. URL https://techcrunch.com/2024/09/26/starlink-will-hit-4-million-subscribers-this-week-spacex-president-says/. Accessed: 2024-11-17.

[35] Jonathan McDowell. Starlink statistics. URL https://planet4589.org/space/con/star/stats.html. Accessed: 2024-11-17.

[36] Ridhima Sawhney and Rohit Singh. Future use of v-band in satellite communication. *International Journal of Latest Trends in Engineering and Technology*, 7(3):205–210, 2024. ISSN 2278-621X. doi: 10.21172/1.73.029. URL http://dx.doi.org/10.21172/1.73.029.

[37] Efstratios Ntantis. Space debris: Overview and mitigation strategies, 2024. URL https://www.researchgate.net/profile/Efstratios-Ntantis/publication/378802933_Space_Debris_Overview_and_mitigation_strategies/links/666af1a5a54c5f0b946463e3/. Accessed: November 2024.